*The 2015 World Congress on*
***Advances in Civil, Environmental, and Materials Research (ACEM15)***
*Incheon, Korea, August 25-29, 2015*

# Design feasibility of double-skinned composite tubular wind turbine tower

*Taek Hee Han[1)], Gil-Lim Yoon[1)], Jin-Hak Yi[1)] and Deokhee Won[2)]

[1), 2)] *Coastal Development & Ocean Energy Research Division, Korea Institute of Ocean Science and Technology, Ansan 426-744, Republic of Korea*
[1)] *taekheehan@kiost.ac.kr*

## ABSTRACT

A double-skinned composite tubular (DSCT) wind power tower was suggested and automatic section design software was developed. The developed software adopted the nonlinear material model and the nonlinear column model. If the outer diameter, material properties and design capacities of a DSCT wind power tower are given, the developed software performs axial force-bending moment interaction analyses for hundreds of sections of the tower and suggests ten optimized cross-sectional designs. In this study, 80 sections of DSCT wind power towers were designed for 3.6MW and 5.0MW turbines. And the performances of the designed 80 sections were analyzed with and without considerations of large displacement effect. In designing and analyzing them, the material nonlinearity and the confining effect of concrete considered. The comparison of the analysis results showed the moment capacity loss of the wind power tower by the mass of the turbine is significant and the large displacement effect should be considered for the safe design of the wind power tower.

## 1. INTRODUCTION

By high energy prices and supply uncertainties, many countries are trying to develop renewable energies such as wind power, tidal power, geothermal power and photovoltaic power. Among them, wind power is evaluated to have the best energy efficiency. Several offshore wind farms are planned and have been constructed over the world. According to GWEC (Global Wind Energy Council), the installed wind turbines reach to 282,430MW in the world until 2012. The world average annual growth rate of wind turbine installation from 1996 to 2012 is 27.7% and the annual growth rate in the year of 2012 is 18.7%. Owing to the growth of offshore wind energy market, in 2009, the installation of wind turbine grew from 26,721MW to 38,708MW by 44.8% (Sawyer, 2013).

The offshore wind power started to grow up from 1980's by focusing on the development of offshore wind farms. In 2008, the offshore wind farms generated

[1)] Principal Research Scientist
[2)] Post-Doctoral Researcher

25,413TWh/year. In this time, United Kingdom and several countries in Europe are leading the offshore wind farm construction and operation. Table 1 shows the installed capacity of offshore farm and Table 2 shows the offshore wind farm development plan of South Korea.

Table 1 Top 10 EU Countries in Offshore Wind Power (Sawyer, 2013)

| Country | No. of farms | No. of turbines | Capacity installed (MW) |
|---|---|---|---|
| UK | 20 | 870 | 2,947.9 |
| Denmark | 12 | 416 | 921.0 |
| Belgium | 2 | 91 | 379.5 |
| Germany | 6 | 68 | 280.3 |
| Netherlands | 4 | 124 | 246.8 |
| Sweden | 6 | 75 | 163.7 |
| Finland | 2 | 9 | 26.3 |
| Ireland | 1 | 7 | 25.2 |
| Norway | 1 | 1 | 2.3 |
| Portugal | 1 | 1 | 2.0 |
| Total | 55 | 1,662 | 4,995 |

Table 2 Offshore Wind Farm Development Plan of Korea (Sung, 2012)

| Plant | Capacity (MW) | Remark |
|---|---|---|
| Southwest Sea | 2,500 | Investigating wind condition |
| Jeonnam | 4,000 | Investigating wind condition |
| Sam-Mu | 30 | '12.7 (constructing) |
| Daejeong | 200 | Design process |
| Han-Lim | 150 | Investigating wind condition |
| Haengwon | 60 | Design process |
| Total | 6,940 | |

Because of better wind quality on offshore than onshore, offshore wind farm increases and the generating turbines, blades, and towers are getting bigger and taller. However, as the tower becomes taller, its slenderness ratio increases. This large slenderness ratio makes a tower easy to be buckled or to fail as shown in Fig. 1. Therefore, to reduce the failure possibility of a tall tower, a new-type tower structure, which has high strength, is necessary. In this study, a double-skinned concrete filled tube (DSCT) was adopted as the wind power tower to enhance the load resisting capacity of a wind tower. And automatic section design software of a DSCT wind power tower was developed based on the nonlinear material model (Han et al., 2010) and the

nonlinear column model (Han et al., 2013) considering the confining effect of concrete. By using the developed software, the section design and performance analysis for the DSCR wind power tower were carried out. The designed DSCT tower was set to satisfy the required capacities to support 3.6MW and 5.0MW turbines, which were supported by the reference steel wind power towers.

Fig. 1 Failure of steel wind tower (Khatri, 2013; http://galleryhip.com; Ruralgrubby's Wind Watch)

## 2. AUTOMATIC DESIGN PROGRAM FOR DSCT TOWER

### *2.1 DSCT Column*

A DSCT column was introduced by Shakir-Khalil and Illouli in 1987. It is a column composed of two concentric tubes and concrete between them as shown in Fig. 2. After their introduction, the axial strength of the DSCT column was studied (Wei et al., 1995; Zhao and Grzebieta, 2002; Tao et al., 2004) and it was reported that the axial strength of a DSCT column was larger than the sum of axial strengths from the inner tube, outer tube, and concrete (Wei et al., 1995). Recently, a hybrid DSCT column, which is composed of fiber, reinforced polymer (FRP) tubes and concrete, has been studied (Teng et al., 2006; Yu et al., 2006). Han et al. (2010; 2013) proposed the material nonlinear model and column model of a DSCT column and studied the bending strength of a DSCT column.

In this study, an automatic section design program for a DSCT tower was coded with FORTRAN language. It is based on the nonlinear model of a DSCT column (Han et al., 2013). The strain compatibility of a DSCT tower is derived from the section analysis as shown in Fig. 3, and the relation of curvature and lateral displacement is defined from Fig. 4. The column model uses a section analysis and adopted the layer-by-layer technique for numerical integration of stresses (Kilpatrick and Ranagan, 1997). The stresses in the layers of the concrete and the tubes are calculated as the change

of strain. Axial loads and moments for the concrete and the tubes are given as Eqs. 1~8 (Han et al., 2013).

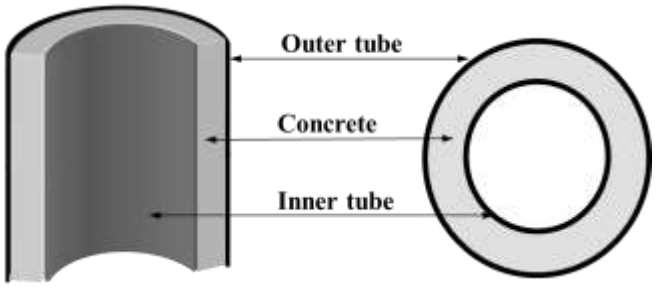


Fig. 2 Cross section of DSCT column

$$P_i^{CC} = \sum_{j=1}^{n} P_{i,j}^{CC} = \sum_{j=1}^{n} A_{i,j}^{CC} \cdot f_{i,j}^{CC} \quad (1)$$

$$P_i^{IT} = \sum_{j=1}^{n} P_{i,j}^{IT} = \sum_{j=1}^{n} A_{i,j}^{IT} \cdot f_{i,j}^{IT} \quad (2)$$

$$P_i^{OT} = \sum_{j=1}^{n} P_{i,j}^{OT} = \sum_{j=1}^{n} A_{i,j}^{OT} \cdot f_{i,j}^{OT} \quad (3)$$

$$M_i^{CC} = \sum_{j=1}^{n} M_{i,j}^{CC} = \sum_{j=1}^{n} P_{i,j}^{CC} \cdot x_{i,j}^{CC} \quad (4)$$

$$M_i^{IT} = \sum_{j=1}^{n} M_{i,j}^{IT} = \sum_{j=1}^{n} P_{i,j}^{IT} \cdot x_{i,j}^{IT} \quad (5)$$

$$M_i^{OT} = \sum_{j=1}^{n} M_{i,j}^{OT} = \sum_{j=1}^{n} P_{i,j}^{OT} \cdot x_{i,j}^{OT} \quad (6)$$

$$P_i = P_i^{CC} + P_i^{IT} + P_i^{OT} \quad (7)$$

$$M_i = M_i^{CC} + M_i^{IT} + M_i^{OT} \quad (8)$$

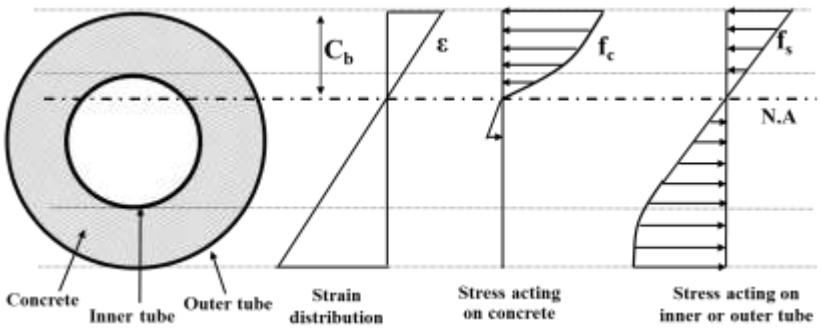


Fig. 3 Section analysis using strain compatibility and layer-by-layer approach (Han et al., 2013)

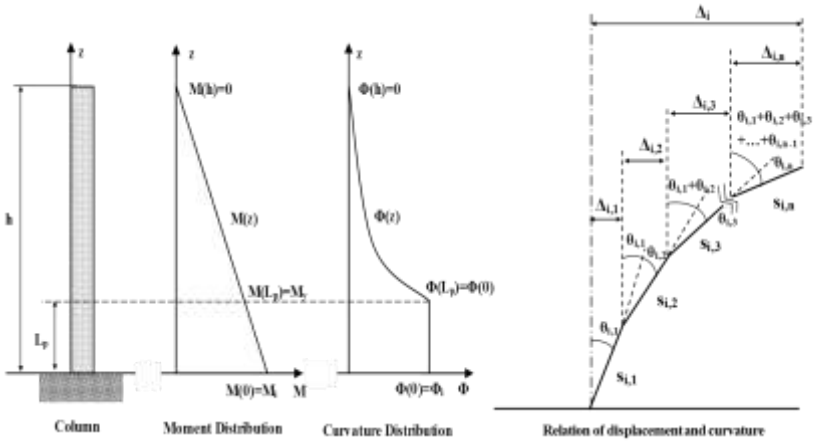


Fig. 4 Curvature and displacement functions (Han et al., 2013)

If the column is divided to numerous small elements along its height, the curvature corresponding to the each element can be calculated from the curvature function (Han et al., 2013). Fig. 4 shows the column composed of a certain numbers of elements which have the length of $S_{i,j}$. The rotation angle is given as Eq. (9) from the curvature function. The lateral displacement of the top point of the column can be calculated by summating the lateral displacements of all elements in the stage of the strain distribution as Eq. (10) (Han et al., 2013).

$$\theta_{i,j} = \phi(z) \cdot S_{i,j} \tag{9}$$

$$\Delta_i = \sum_{j=1}^{n} \Delta_{i,j} = \sum_{j=1}^{n} \left( S_{i,j} \sum_{k=1}^{j} \theta_{i,k} \right) \tag{10}$$

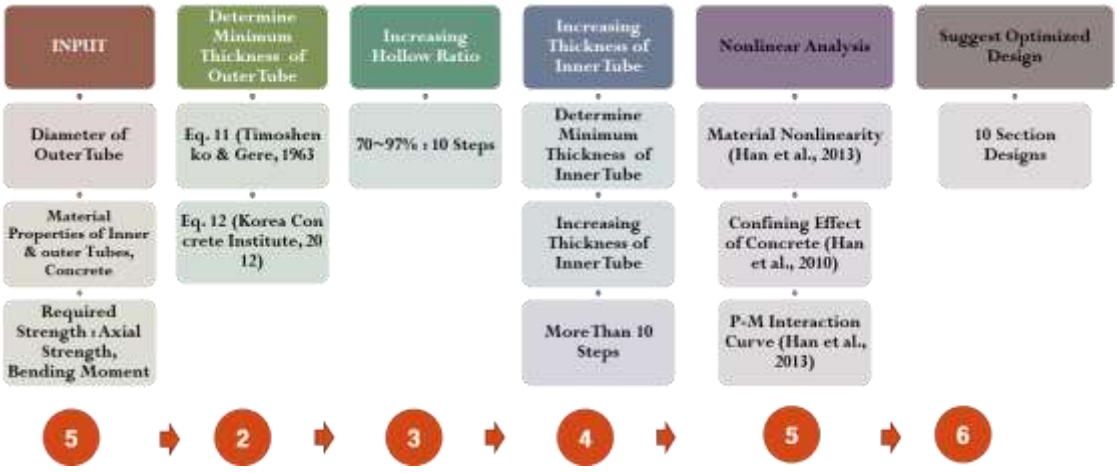


Fig. 5 Design process in developed programs

### *2.2 Automatic Design Program*

The developed design program, Auto DSCT® (Han, 2014), performs the section design of a DSCT tower in the procedure as shown in Fig. 5. The program performs axial load-bending moment (P-M) interaction and lateral force-lateral displacement (P-Δ) analyses when it is given the input data which contains the outer diameter, the material properties, the required bending moment and axial strength of a DSCT tower. During the analysis, it varies the hollow ratio, the thicknesses of the inner tube, and the thicknesses of the outer tube. As the results, the program shows ten optimum design sections which satisfy the required capacities. The program calculates minimum thickness of the outer tube which satisfies Eq. (11) (Timoshenko and Gere, 1936) and Eq. (12) (Korea Concrete Institute, 2012) to avoid its local buckling failure.

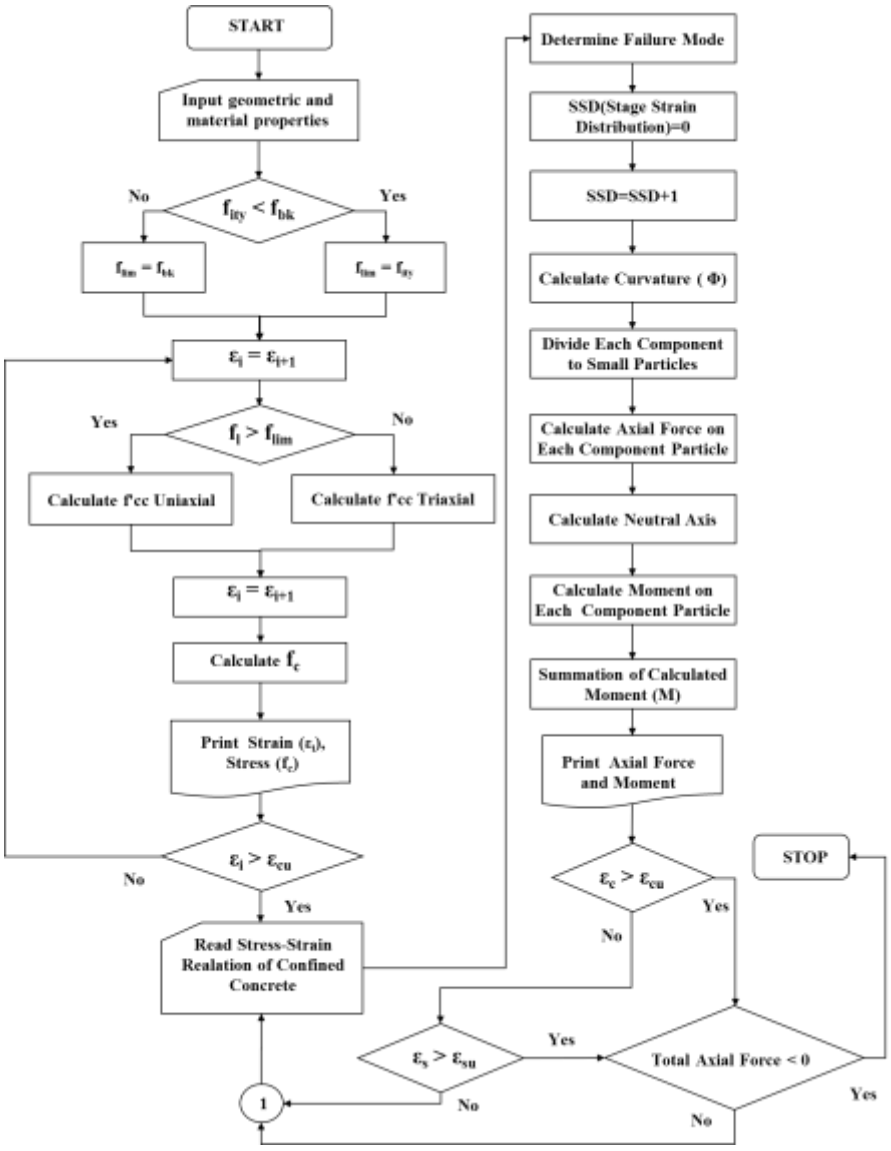


Fig. 6 Flowchart of P-M interaction analysis

$$f_{cr} = \frac{t \cdot E_t}{\frac{D}{2}\sqrt{3(1-\nu^2)}} \tag{11}$$

$$t > (D+t)\sqrt{\frac{f_y}{8E}} \tag{12}$$

$$t_i > \frac{D_i \cdot f_y \cdot t}{D \cdot f_{iy}} \tag{13}$$

$$t_i = \sqrt{\frac{6D_i^2 \cdot f_y \cdot t}{2.27D \cdot E_i}} \tag{14}$$

After determination of the thickness of the outer tube, the hollow ratio of the DSCT tower decreases from 97% to 70% by the step of 3%. The thickness of the inner tube is calculated to satisfy Eq. (13) and Eq. (14) simultaneously (Han et al., 2010), and the P-M interaction analysis is performed increasing the thickness of the inner tube by 0.01mm. The design procedure is as shown in Fig. 5, and the P-M interaction analysis, which considers the material nonlinearity and the confining effect of concrete, is performed as the flow in Fig. 6. The proposed optimum ten design sections have the thinnest tubes among the given hollow ratio. Because the ten design sections have different hollow ratio, their axial strength and bending strength are different. Therefore, engineers can select one which is proper to their design purpose.

## 3. AUTOMATIC DESIGN OF DSCT WIND POWER TOWER

In this study, the design of steel wind power towers, which were built in Kriegers Flak Offshore Wind Farm (Ljjj and Gravesen, 2008) as shown in Fig. 7, were referred to perform automatic design of DSCT wind power towers. 3.6MW and 5.0MW turbines were installed in Kriegers Flak Offshore Wind Farm and the dimensions of reference steel towers are summarized in Table 3. As shown in Table 3, the bottom diameters and wall thicknesses of the steel towers are 4.5m and 30mm for the 3.6MW turbine; 6.0m and 35mm for the 5.0MW turbine, respectively. Table 4 shows design vertical loads, extreme loads, operational loads, and fatigue loads which were applied to the steel towers supporting 3.6MW and 5.0MW turbines. To design DSCT wind power towers, vertical load and extreme bending moment ($M_{ex}$), which were the largest values in Table 4, were selected and applied as the required axial strength and bending strength. The automatic design was performed for two types of DSCT towers. One had steel tubes and the other had FRP tubes. The DSCT towers were set to have smaller diameters than steel towers and to satisfy the design loads which applied to the steel towers.

Table 3 Reference Turbines and Steel Towers (Ljjj and Gravesen, 2008)

| Turbine size | 3.6 MW | 5 MW |
|---|---|---|
| Output power | 3.6MW | 5.0MW |
| Rotor diameter | 106m | 126m |
| Foundation–tower interface level acc. MSL* | 3.5m | 3.5m |
| Hub height above foundation interface | 72.5m | 82.5m |
| Nacelle mass incl. Rotor | 220tons | 410 tons |
| Tower top diameter/wall thickness | 3.5m/15mm | 4.5m/20mm |
| Tower bottom diameter/wall thickness | 4.5m/30mm | 6.0m/35mm |
| Tower mass | 220tons | 300tons |

*MSL: Mean Sea Level

Table 4. Turbine Loads (Ljjj and Gravesen, 2008)

| Turbine Design load | | Vertical load (MN) | Extreme load | | Operational load | | Fatigue load m=(4-5) N:$1 \times 10^7$ | |
|---|---|---|---|---|---|---|---|---|
| Capacity | Level | | $F_{ex}$ | $M_{ex}$ | $F_{op}$ | $M_{op}$ | $F_{eq}$ | $M_{eq}$ |
| 3.6 MW | 15 m | 4.40 | 1.42 MN | 89.90 MN-m | 0.85 MN | 54.0 MN-m | 0.35 MN | 19.20 MN-m |
| 5.0 MW | 15 m | 7.10 | 2.03 MN | 150.00 MN-m | 1.20 MN | 90.0 MN-m | 0.49 MN | 28.10 MN-m |

Automatic design processes were performed for the DSCT towers. The required axial strength and bending strength were 4.40MW and 89.9MN-m for 3.6MW turbine and 7.10MN and 150.00MN-m for 5.0MW turbine, respectively. The DSCT towers were set to have smaller diameters than the reference steel towers. The design case of DSCT tower had 8 different diameters, which were 95%, 80%, 65%, and 50% of the reference steel towers for 3.6MW and 5.0MW turbines. Table 5 shows the design cases of DSCT towers. In the design of DSCT towers, the strength of concrete was 29.43MPa; the yield strength and ultimate strength of the steel tube were 313.60MPa and 490.50MPa, respectively.

Fig. 7 Map of the western Baltic Sea south of Sweden and the site (Ljjj and Gravesen, 2008)

Table 5 Design Case of DSCT Tower with Steel Tubes

| Turbine size | Diameter Ratio* | Diameter | Design Case** |
|---|---|---|---|
| 3.6MW Steel Tube DSCT Tower | 0.95 | 4,275mm | 3S95 |
| | 0.90 | 4,050mm | 3S90 |
| | 0.85 | 3,825mm | 3S85 |
| | 0.80 | 3,600mm | 3S80 |
| 5.0MW Steel Tube DSCT Tower | 0.95 | 5,700mm | 5S95 |
| | 0.90 | 5,400mm | 5S90 |
| | 0.85 | 5,100mm | 5S85 |
| | 0.80 | 4,800mm | 5S80 |

Diameter Ratio*: Diameter of DSCT Wind Tower / Diameter of Steel Wind Tower
Design Case**: tSd (eg, 3S95, 5S80), t=turbine capacity, S=steel tube, d=diameter ratio($\times 10^{-2}$)

The designed sections of DSCT towers, which were recommended by the developed program for the 3.6MW and 5.0MW turbines, are summarized in Tables 6 and 7, respectively. The recommended design cases are the most economic sections at the each hollow ratio ($D_i/D$) because they have the smallest thicknesses of the inner and outer tubes. When the hollow ratio decreases, the thicknesses of the inner and outer tubes decrease. This means that a DSCT tower with a large hollow ratio requires much concrete but less steel. Fig. 6 and Fig. 7 show P-M interaction curves of the designed DSCT towers. Fig. 8 and Fig. 9 show P-M interaction curves of the designed DSCT towers.

Table 6 Recommended Section Design for 3.6MW DSCT Wind Tower

| Design Case for 3S95 | 3S95/97 | 3S95/94 | 3S95/91 | 3S95/88 | 3S95/85 | 3S95/82 | 3S95/79 | 3S95/76 | 3S95/73 | 3S95/70 |
|---|---|---|---|---|---|---|---|---|---|---|
| $D$ (mm) | 4275.0 | 4275.0 | 4275.0 | 4275.0 | 4275.0 | 4275.0 | 4275.0 | 4275.0 | 4275.0 | 4275.0 |
| $D_i$ (mm) | 4146.8 | 4018.5 | 3890.3 | 3762.0 | 3633.8 | 3505.5 | 3377.3 | 3249.0 | 3120.8 | 2992.5 |
| $D_i / D$ | 0.97 | 0.94 | 0.91 | 0.88 | 0.85 | 0.82 | 0.79 | 0.76 | 0.73 | 0.70 |
| $t$ (mm) | 5.50 | 5.50 | 5.50 | 5.50 | 5.50 | 5.50 | 5.50 | 5.50 | 5.50 | 5.50 |
| $t_i$ (mm) | 10.38 | 10.06 | 9.74 | 9.42 | 9.09 | 8.77 | 8.45 | 8.13 | 7.81 | 7.49 |
| Design Case for 3S90 | 3S90/97 | 3S90/94 | 3S90/91 | 3S90/88 | 3S90/85 | 3S90/82 | 3S90/79 | 3S90/76 | 3S90/73 | 3S90/70 |
| $D$ (mm) | 4050.0 | 4050.0 | 4050.0 | 4050.0 | 4050.0 | 4050.0 | 4050.0 | 4050.0 | 4050.0 | 4050.0 |
| $D_i$ (mm) | 3928.5 | 3807.0 | 3685.5 | 3564.0 | 3442.5 | 3321.0 | 3199.5 | 3078.0 | 2956.5 | 2835.0 |
| $D_i / D$ | 0.97 | 0.94 | 0.91 | 0.88 | 0.85 | 0.82 | 0.79 | 0.76 | 0.73 | 0.70 |
| $t$ (mm) | 5.50 | 5.50 | 5.50 | 5.50 | 5.50 | 5.50 | 6.00 | 6.00 | 6.50 | 6.50 |
| $t_i$ (mm) | 10.10 | 9.79 | 9.48 | 9.16 | 8.85 | 8.54 | 8.59 | 8.27 | 8.26 | 7.93 |
| Design Case for 3S85 | 3S85/97 | 3S85/94 | 3S85/91 | 3S85/88 | 3S85/85 | 3S85/82 | 3S85/79 | 3S85/76 | 3S85/73 | 3S85/70 |
| $D$ (mm) | 3825.0 | 3825.0 | 3825.0 | 3825.0 | 3825.0 | 3825.0 | 3825.0 | 3825.0 | 3825.0 | 3825.0 |
| $D_i$ (mm) | 3710.3 | 3595.5 | 3480.8 | 3366.0 | 3251.3 | 3136.5 | 3021.8 | 2907.0 | 2792.3 | 2677.5 |
| $D_i / D$ | 0.97 | 0.94 | 0.91 | 0.88 | 0.85 | 0.82 | 0.79 | 0.76 | 0.73 | 0.70 |
| $t$ (mm) | 6.50 | 6.00 | 6.00 | 6.00 | 6.50 | 6.50 | 7.00 | 7.50 | 7.50 | 8.00 |
| $t_i$ (mm) | 10.67 | 9.94 | 9.62 | 9.30 | 9.35 | 9.02 | 9.02 | 8.98 | 8.63 | 8.54 |
| Design Case for 3S80 | 3S80/97 | 3S80/94 | 3S80/91 | 3S80/88 | 3S80/85 | 3S80/82 | 3S80/79 | 3S80/76 | 3S80/73 | 3S80/70 |
| $D$ (mm) | 3600.0 | 3600.0 | 3600.0 | 3600.0 | 3600.0 | 3600.0 | 3600.0 | 3600.0 | 3600.0 | 3600.0 |
| $D_i$ (mm) | 3492.0 | 3384.0 | 3276.0 | 3168.0 | 3060.0 | 2952.0 | 2844.0 | 2736.0 | 2628.0 | 2520.0 |
| $D_i / D$ | 0.97 | 0.94 | 0.91 | 0.88 | 0.85 | 0.82 | 0.79 | 0.76 | 0.73 | 0.70 |
| $t$ (mm) | 8.00 | 7.50 | 7.50 | 7.50 | 8.00 | 8.00 | 8.50 | 8.50 | 9.00 | 9.50 |
| $t_i$ (mm) | 11.49 | 10.78 | 10.43 | 10.09 | 10.07 | 9.71 | 9.64 | 9.28 | 9.17 | 9.03 |

Table 7 Recommended Section Design for 5.0MW DSCT Wind Tower

| Design Case for 5S95 | 5S95/97 | 5S95/94 | 5S95/91 | 5S95/88 | 5S95/85 | 5S95/82 | 5S95/79 | 5S95/76 | 5S95/73 | 5S95/70 |
|---|---|---|---|---|---|---|---|---|---|---|
| $D$ (mm) | 5700.0 | 5700.0 | 5700.0 | 5700.0 | 5700.0 | 5700.0 | 5700.0 | 5700.0 | 5700.0 | 5700.0 |
| $D_i$ (mm) | 5529.0 | 5358.0 | 5187.0 | 5016.0 | 4845.0 | 4674.0 | 4503.0 | 4332.0 | 4161.0 | 3990.0 |
| $D_i / D$ | 0.97 | 0.94 | 0.91 | 0.88 | 0.85 | 0.82 | 0.79 | 0.76 | 0.73 | 0.70 |
| $t$ (mm) | 7.50 | 7.50 | 7.50 | 7.50 | 7.50 | 7.50 | 7.50 | 7.50 | 7.50 | 7.50 |
| $t_i$ (mm) | 13.99 | 13.56 | 13.13 | 12.70 | 12.26 | 11.83 | 11.40 | 10.96 | 10.53 | 10.10 |
| Design Case for 5S90 | 5S90/97 | 5S90/94 | 5S90/91 | 5S90/88 | 5S90/85 | 5S90/82 | 5S90/79 | 5S90/76 | 5S90/73 | 5S90/70 |
| $D$ (mm) | 5400.0 | 5400.0 | 5400.0 | 5400.0 | 5400.0 | 5400.0 | 5400.0 | 5400.0 | 5400.0 | 5400.0 |
| $D_i$ (mm) | 5238.0 | 5076.0 | 4914.0 | 4752.0 | 4590.0 | 4428.0 | 4266.0 | 4104.0 | 3942.0 | 3780.0 |
| $D_i / D$ | 0.97 | 0.94 | 0.91 | 0.88 | 0.85 | 0.82 | 0.79 | 0.76 | 0.73 | 0.70 |
| $t$ (mm) | 7.00 | 7.00 | 7.00 | 7.00 | 7.00 | 7.00 | 7.00 | 7.00 | 7.00 | 7.00 |
| $t_i$ (mm) | 13.16 | 12.75 | 12.35 | 11.94 | 11.53 | 11.12 | 10.72 | 10.31 | 9.90 | 9.50 |
| Design Case for 5S85 | 5S85/97 | 5S85/94 | 5S85/91 | 5S85/88 | 5S85/85 | 5S85/82 | 5S85/79 | 5S85/76 | 5S85/73 | 5S85/70 |
| $D$ (mm) | 5100.0 | 5100.0 | 5100.0 | 5100.0 | 5100.0 | 5100.0 | 5100.0 | 5100.0 | 5100.0 | 5100.0 |
| $D_i$ (mm) | 4947.0 | 4794.0 | 4641.0 | 4488.0 | 4335.0 | 4182.0 | 4029.0 | 3876.0 | 3723.0 | 3570.0 |
| $D_i / D$ | 0.97 | 0.94 | 0.91 | 0.88 | 0.85 | 0.82 | 0.79 | 0.76 | 0.73 | 0.70 |
| $t$ (mm) | 6.50 | 6.50 | 6.50 | 6.50 | 6.50 | 6.50 | 6.50 | 6.50 | 6.50 | 6.50 |
| $t_i$ (mm) | 12.32 | 11.94 | 11.56 | 11.18 | 10.80 | 10.42 | 10.04 | 9.66 | 9.27 | 8.89 |
| Design Case for 5S80 | 5S80/97 | 5S80/94 | 5S80/91 | 5S80/88 | 5S80/85 | 5S80/82 | 5S80/79 | 5S80/76 | 5S80/73 | 5S80/70 |
| $D$ (mm) | 4800.0 | 4800.0 | 4800.0 | 4800.0 | 4800.0 | 4800.0 | 4800.0 | 4800.0 | 4800.0 | 4800.0 |
| $D_i$ (mm) | 4656.0 | 4512.0 | 4368.0 | 4224.0 | 4080.0 | 3936.0 | 3792.0 | 3648.0 | 3504.0 | 3360.0 |
| $D_i / D$ | 0.97 | 0.94 | 0.91 | 0.88 | 0.85 | 0.82 | 0.79 | 0.76 | 0.73 | 0.70 |
| $t$ (mm) | 6.50 | 6.50 | 6.50 | 6.50 | 6.50 | 6.50 | 7.00 | 7.00 | 7.50 | 8.00 |
| $t_i$ (mm) | 11.96 | 11.59 | 11.22 | 10.85 | 10.48 | 10.11 | 10.10 | 9.72 | 9.66 | 9.57 |

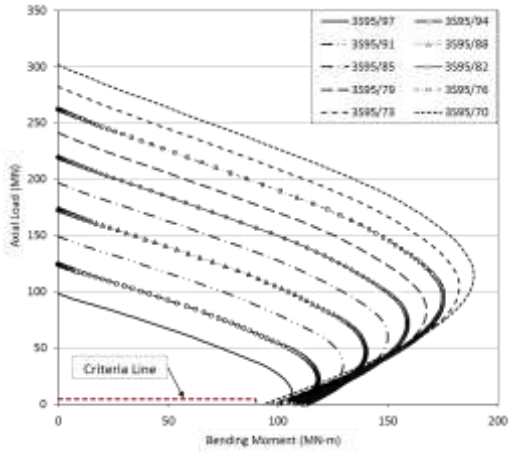


(a) 3S95

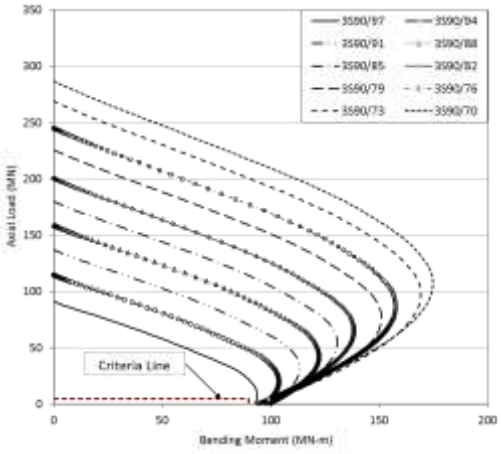


(b) 3S90

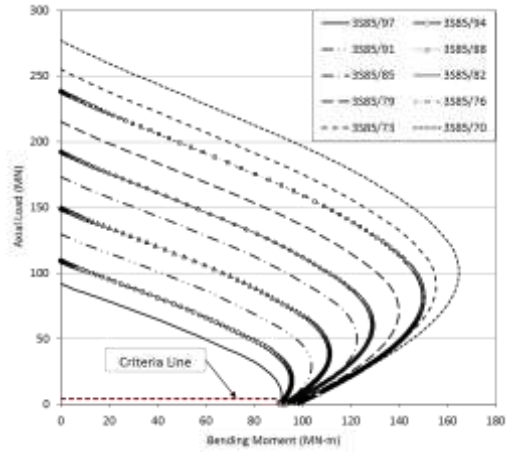


(c) 3S85

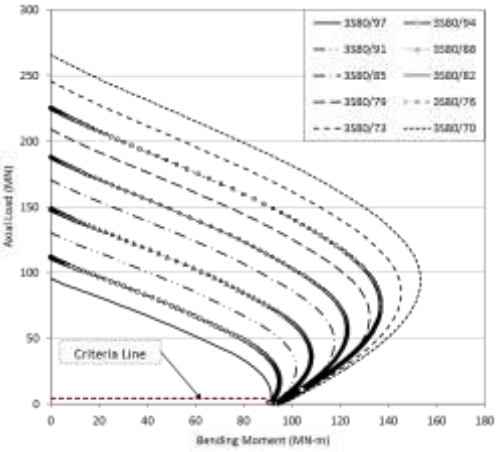


(d) 3S80

Fig. 8 P-M interaction curves of designed DSCT wind towers for 3.6MW turbines

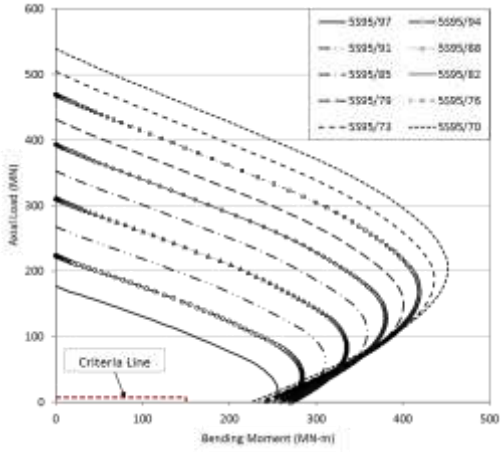


(a) 5S95

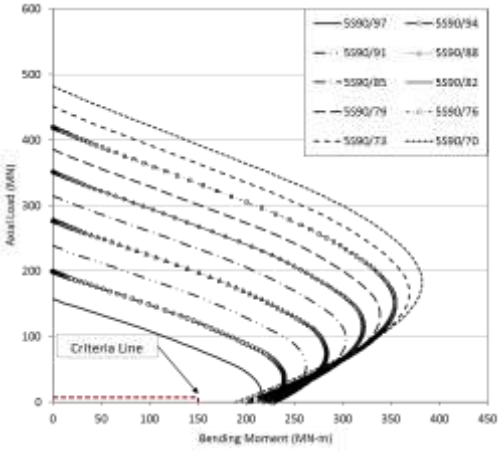


(b) 5S90

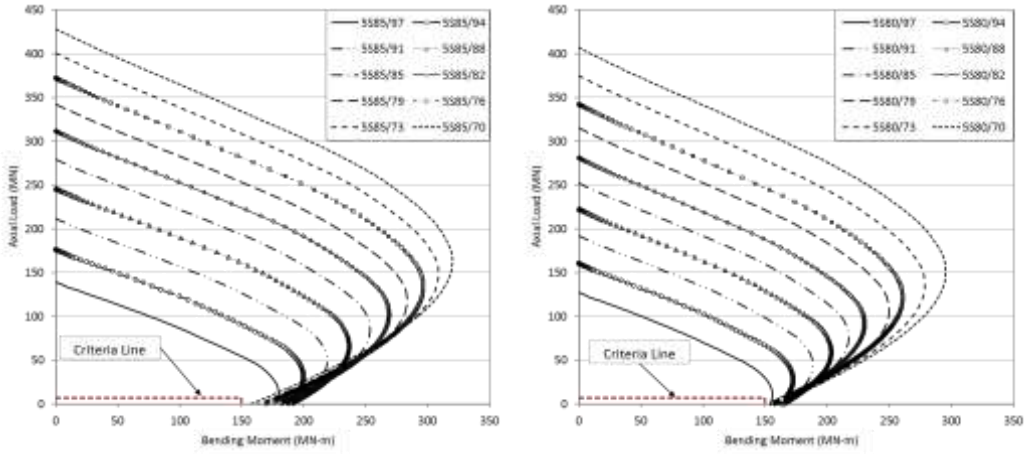


(c) 5S85 (d) 5S80

Fig. 9 P-M interaction curves of designed DSCT wind towers for 5.0MW turbines

## 4. LATERAL BEHAVIOR CONSIDERING LARGE DISAPLACEMENT EFFECT

The mass of wind turbine which is located on the top of a slender wind tower makes additional moment by gravity as the wind tower is bent by the lateral force such wind load. In this case, the lateral displacement is the moment arm of the vertical force by the turbine mass and gravity as shown in Fig. 10. This additional moment makes the tower cannot exert its original moment resisting capacity against the lateral force.

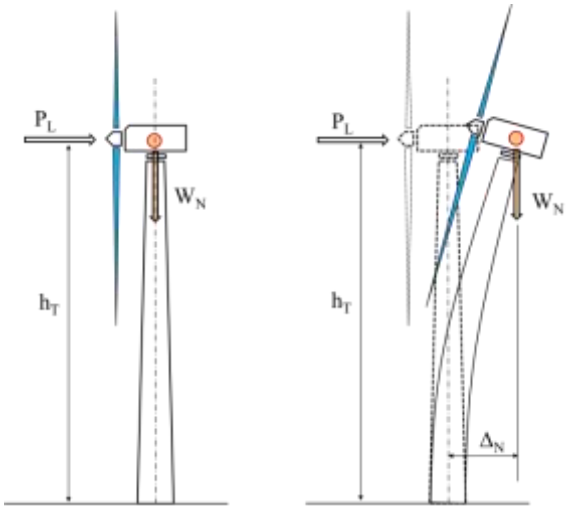


Fig. 10 Consideration of large displacement effect

The moment-displacement relation analyses were performed for the designed 80 DSCT wind towers by CoWiTA® (Han, 2015). In the analyses, material nonlinearity and confining effect of concrete were considered. Following figures show the analysis results and comparison when large displacement effect was considered (LDE) and not considered (SDE). As shown in Fig. 11(a) and Fig. 13(a), all designed sections satisfy the required capacity when the large displacement effect was not considered. However, as shown in Fig. 12 ans Fig. 14, some designed sections may not satisfy the required capacity when the large displacement effect was considered. Therefore, the large displacement effect should be considered for when a slender column such as a wind tower. Fig. 15 shows the reduced moment ratios of the designed DSCT towers by considering large displacement effect. As shown in the figure, the tower with large slenderness ratio loses more moment capacity up to 33% (5S80 with 97% hollow ratio).

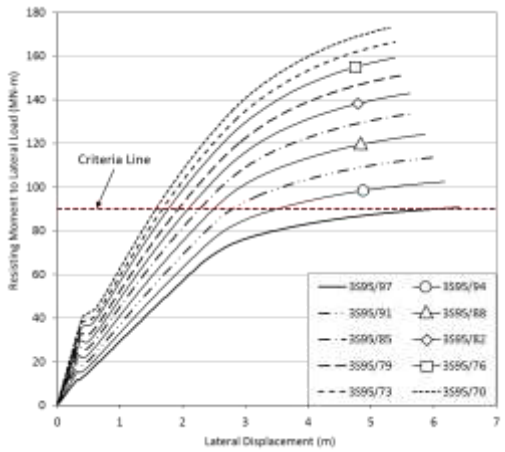


(a) 3S95 (SDE)

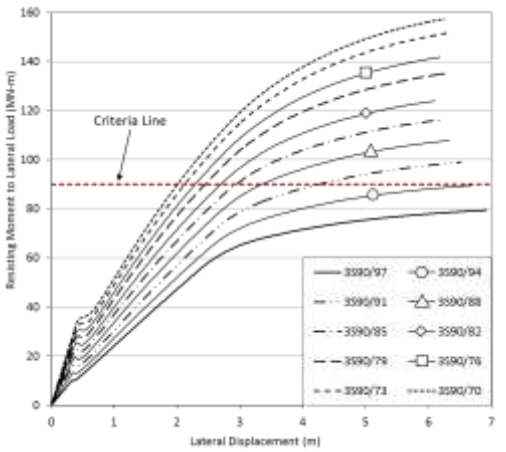


(b) 3S90 (SDE)

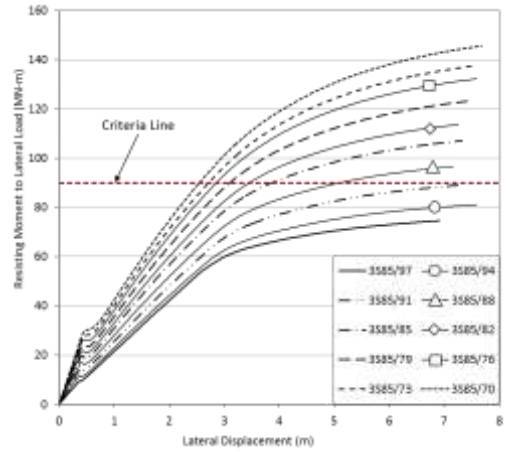


(c) 3S85 (SDE)

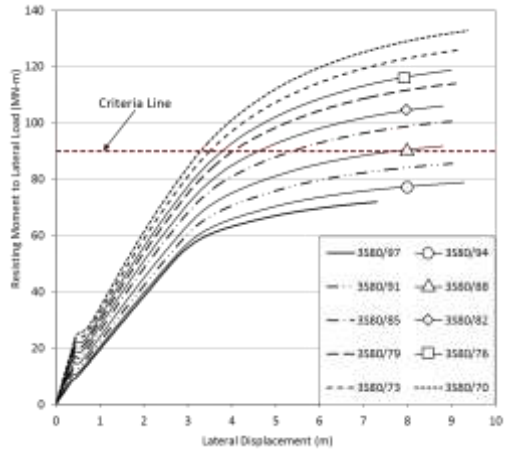


(d) 3S80 (SDE)

Fig. 11 Moment resisting capacity of designed DSCT towers for 3.6MW (SDE)

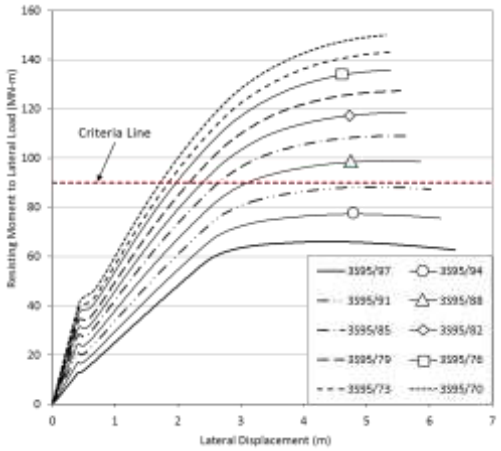


(a) 3S95 (LDE)

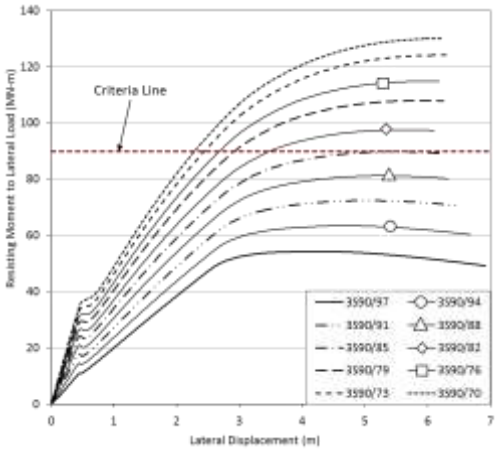


(b) 3S90 (LDE)

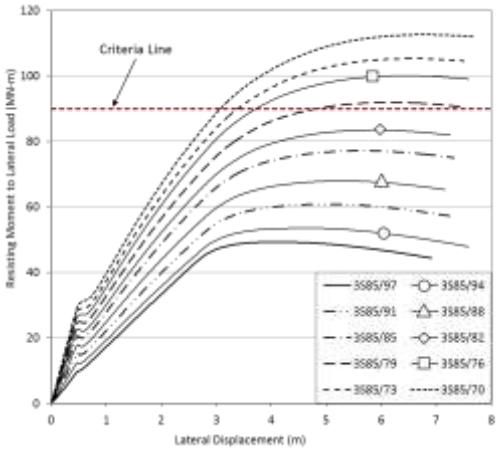


(c) 3S85 (LDE)

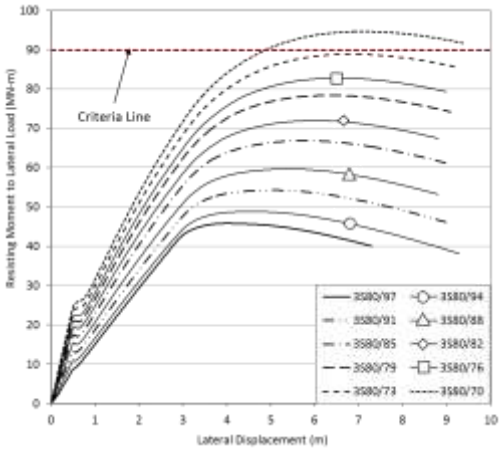


(d) 3S80 (LDE)

Fig. 12 Moment resisting capacity of designed DSCT towers for 3.6MW turbines (LDE)

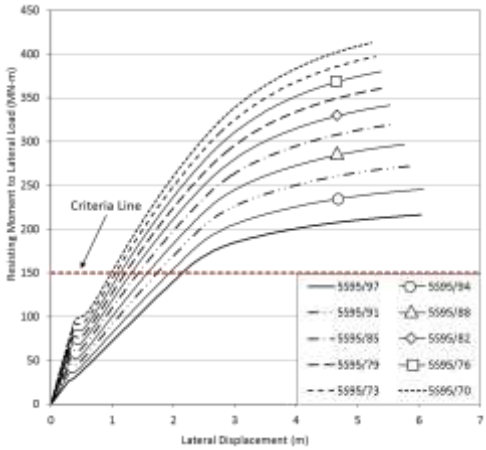


(a) 5S95 (SDE)

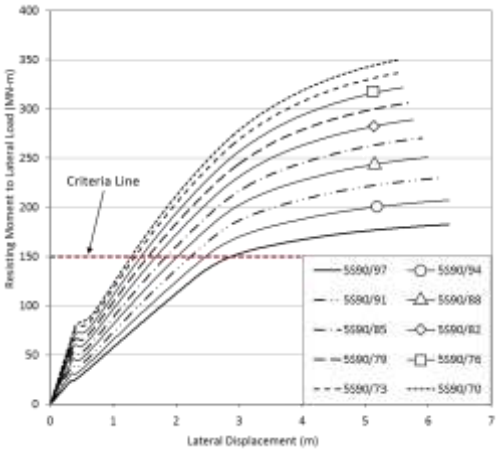


(b) 5S90 (SDE)

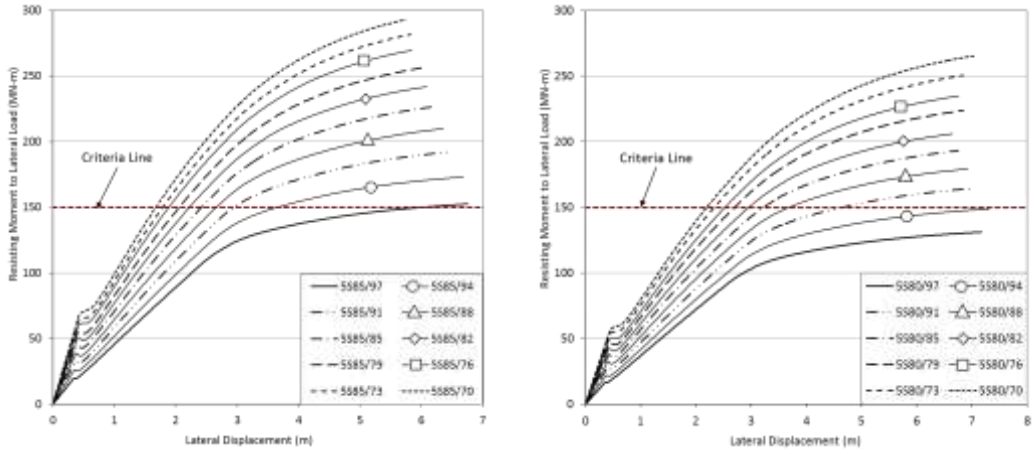


(c) 5S85 (SDE) (d) 5S80 (SDE)

Fig. 13. Moment resisting capacity of designed DSCT towers for 5.0MW (SDE)

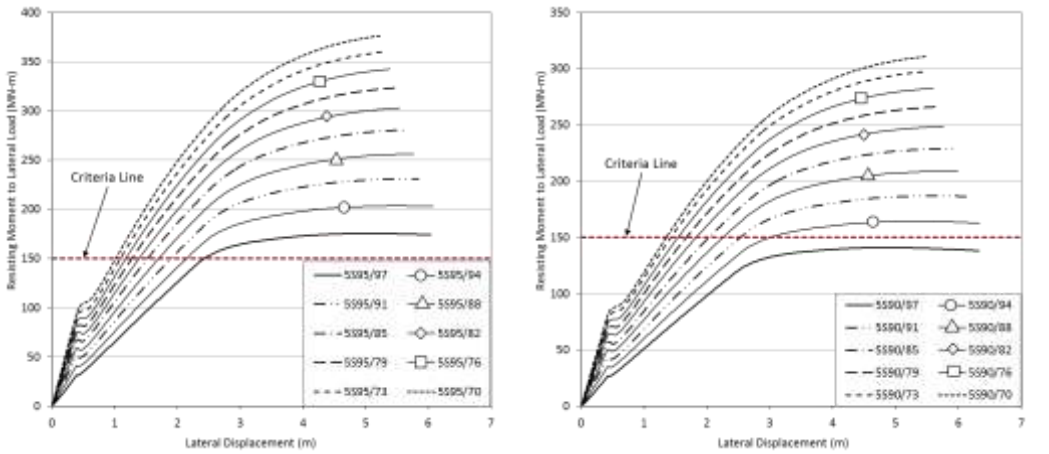


(a) 5S95 (LDE) (b) 5S90 (LDE)

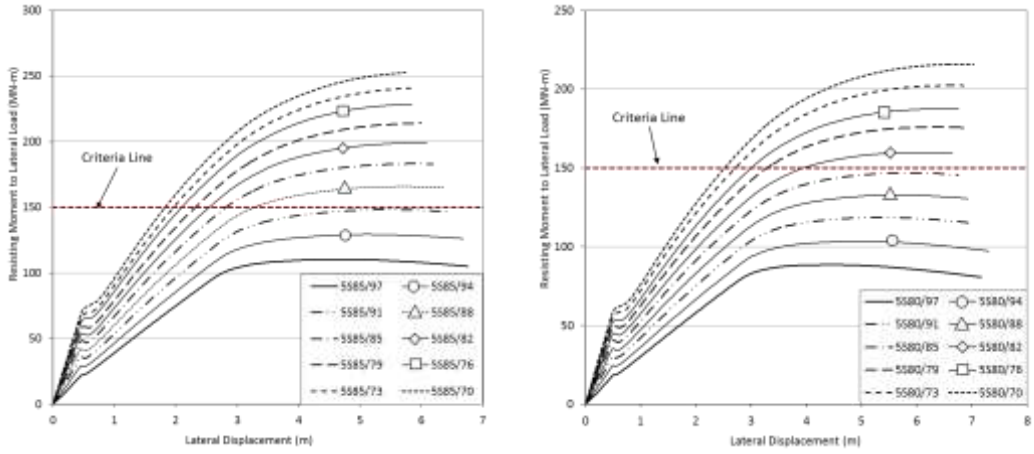


(c) 5S85 (LDE) (d) 5S80 (LDE)

Fig. 14 Moment resisting capacity of designed DSCT towers for 5.0MW (LDE)

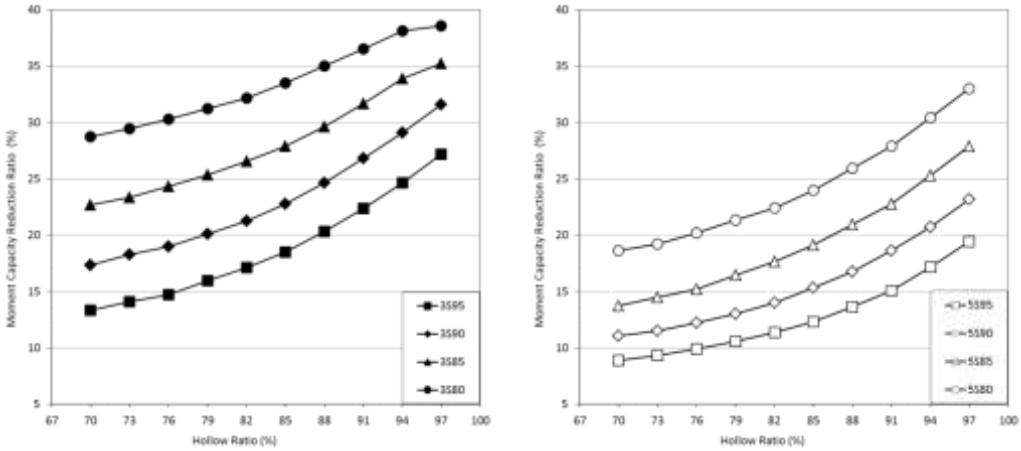


(a) 3.6MW (b) 5.0MW

Fig. 15 Moment Resisting Capacity Reduction Ratio by Large Displacement Effect ($M_W/M_n$)

## 4. CONCLUSIONS

The automatically designed DSCT towers satisfied the required axial and bending strengths. And also, the DSCT towers showed superior performances to the referred steel wind towers although they had smaller diameters. From this result, a DSCT column can be a good candidate for the offshore wind power tower in the future. And the developed design program gave rational design sections.

For the designed DSCT wind towers, performance analyses were carried out with consideration of large displacement effect. Analysis results showed the designed sections were reasonable but large displacement effect makes the slender tower to lose much of its moment resisting capacity. Therefore, for the safety, large displacement effect should be considered in designing wind power towers.

## Acknowledgments

This research was financially supported by the Ministry of Land, Infrastructure and Transport (MOLIT) of the Korea government (code 12 Technology Innovation E09) and Korea Institute of Ocean Science & Technology (project no. PE99323).

## REFERENCES

Galleryhip, website: http://galleryhip.com

Han, T.H. (2014), *Auto DSCT manual Ver. 1.1*, Korea Institute of Ocean Science and Technology, Ansan, Korea.

Han, T.H. (2015), *CoWiTA manual Ver. 2.1*, Korea Institute of Ocean Science and Technology, Ansan, Korea.

Han, T.H., Stallings, J.M. and Kang, Y.J. (2010), “Nonlinear Concrete Model for Double-Skinned Composite Tubular Columns”, *Construction and Building Materials, Elsevier*, **4**(12), 2542-2553.

Han, T.H., Won, D.H., Kim, S. and Kang, Y.J. (2013), "Performance of A DSCT Column under Lateral Loading: Analysis", *Magazine of Concrete Research, Thomas Telford*, **65**(2), 121-135.

Khatri, D. (2013) "As Towers Grow Taller, Consider Structural Impacts", *North American Windpower*, 10(7), 7-11.

Kilpatrick A.E. and Ranagan B.V. (1997), *Deformation-control analysis of composite concrete columns*, Research Report No. 3/97, School of Civil Engineering, Curtin University of Technology, Perth, Western Australia.

Korea Concrete Institute (2012), *Concrete Structure Design Code*, Seoul.

Ljjj L.B.J. and Gravesen, H. (2008), *Kriegers Flak Offshore Wind Farm - Design Basis Foundations*, Vattenfall Vindkraft AB.

Ruralgrubby's Wind Watch, website: http://ruralgrubby.wordpress.com

Sawyer, S. (2013), "Global Wind Power Overview", *Wind Energy Asia*, 76-90.

Shakir-Khalil, H. and Illouli, S, (1987) "Composite columns of concentric steel tubes". *Proceeding of Conference on the Design and Construction of Non-Conventional Structures*, 73-82.

Sung, J.K. (2012), "Current Status of Wind Power Industry and Offshore Wind Projects", *Korea-Europe Wind Plaza 2012*

Tao, Z., Han, L-H. and Zhao, X-L. (2004), "Behavior of concrete-filled double skin (CHS inner and CHS outer) steel tubular stub columns and beam columns", *Journal of Constructional Steel Research*, 60, 1129-1158.

Teng, J.G., Yu, T., Wong, Y.L., and Dong, S.L. (2006), "Hybrid FRP-Concrete-Steel Tubular Columns: Concept and Behavior", *Construction and Building Materials*, 21, 846-854.

Timoshenko, S.P. and Gere, J.M. (1963), *Theory of Elastic Stability, 2nd Edition*, McGraw-Hill, Singapore

Wei, S., Mau, S.T., Vipulanandan, C. and Mantrala, S.K. (1995), "Performance of new sandwich tube under axial loading: Experiment", *Journal of Structural Engineering*, 121, 1806-1814.

Wei, S., Mau, S.T., Vipulanandan, C. and Mantrala, S.K. (1995), "Performance of new sandwich tube under axial loading: Analysis", *Journal of Structural Engineering*, 121, 1815-1821.

Yu, T., Wong, Y.L., Teng, J.G., Dong, S.L., and Lam, E.S.S. (2006), "Flexural Behavior of Hybrid FRP-Concrete-Steel Double-Skin Tubular Members", *Journal of Composites for Construction, ASCE*, 10(5), 443-452.

Zhao, X-L. and Grzebieta, R. (2002), "Strength and ductility of concrete filled double skin (SHS inner and SHS outer) tubes", *Thin-Walled Structures*, 40, 199-213.